New insights on *N-tert*-butyl-α-phenylnitrone † (PBN) as a spin trap. Part 1. Reaction between PBN and *N*-chlorobenzotriazole

Patricia Carloni,[a] Lennart Eberson,*[b] Lucedio Greci,*[a] Paolo Sgarabotto[c] and Pierluigi Stipa[a]

[a] *Dipartimento di Scienze dei Materiali e della Terra, Università di Ancona, via Brecce Bianche, I-60131 Ancona, Italy*
[b] *Department of Chemistry, Lund University, PO Box 124, S-221 00 Lund, Sweden*
[c] *Dipartimento di Chimica Generale ed Inorganica, Chimica Analitica, Chimica Fisica, Università, Centro di Studi per la Strutturistica Diffrattometrica del CNR, Viale delle Scienze, I-43100 Parma, Italy*

_N_-Chlorobenzotriazole (BT–Cl) and _N-tert_-butyl-α-phenylnitrone (PBN) react thermally or photochemically at room temperature with the formation of two isomeric benzotriazolyl spin adducts and the chloro spin adduct, as monitored by EPR spectroscopy. The benzotriazolyl spin adducts are subsequently converted into benzotriazolyl phenyl ketone _O_-benzoyloxime while the latter is converted into the _N_-benzoyl-_N-tert_-butyl aminoxyl radical. Normal solvents do not substantially influence the spin adduct distribution, but the reaction becomes faster in the order of benzene < dichloromethane < acetonitrile. The reaction is autocatalytic in benzotriazole, provided a suitable H atom donor is present, _e.g._ the solvent or added toluene. In 1,1,1,3,3,3-hexafluoropropan-2-ol, a solvent which strongly suppresses nucleophilic processes, only the benzotriazolyl spin adduct is detectable. The macroscale reaction between BT–Cl and PBN confirms the fate of the radicals detected by EPR spectroscopy. The structures of (_Z_)- and (_E_)-benzotriazolyl phenyl ketone _O_-benzoyloxime were determined by X-ray analysis.

Recently, we have studied the reactivity of 1-methyl-2-phenylindole **1** (MPI–H) towards *N*-chlorobenzotriazole **2** (BT–Cl).[1] In the absence of oxygen, the reaction between **1** and **2** afforded ≥90% 3-chloro-1-methyl-2-phenylindole; the radical cations of MPI–H and its 3,3′-connected dehydrodimer, $(MPI)_2$, were detected as transient intermediates. These phenomena were interpreted on the basis of an electron-transfer mechanism which gave rise to the 1-methyl-2-phenylindole radical cation and the BT–Cl radical anion, as shown in reactions (1)–(4). The 1:1 stoichiometry between **1** and **2** suggested that the benzotriazolyl radical formed by cleavage of $BT–Cl^{\bullet -}$ (see below) also acted as a one-electron oxidant toward **1**.

$$BT–Cl + MPI–H \longrightarrow BT–Cl^{\bullet -} + MPI–H^{\bullet +} \quad (1)$$

$$BT–Cl^{\bullet -} \longrightarrow BT^{\bullet} + Cl^{-} \quad (2)$$

$$BT^{\bullet} + MPI–H \longrightarrow BT^{-} + MPI–H^{\bullet +} \quad (3)$$

$$MPI–H^{\bullet +} + Cl^{-} \longrightarrow MPI(H)Cl^{\bullet} \xrightarrow[-H^{+}]{BT–Cl} MPI–Cl \quad (4)$$

In order to obtain additional information on the radical nature of the reaction mechanism, the reaction between MPI–H and BT–Cl was carried out in the presence of *N-tert*-butyl-α-phenylnitrone **3** (PBN) which is a widely used spin trap, well suited for the purpose.[2] However, exploratory experimentation indicated that BT–Cl reacted by itself with PBN to give benzotriazolyl spin adducts in a reaction of some complexity, and we have therefore focused our attention on this process. The results show that the spin adducts are formed according to several mechanisms, and that proper spin trapping of the benzotriazolyl radical by PBN is a minor pathway.

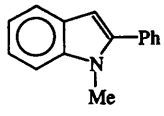

1
MPI-H

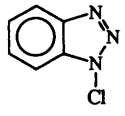

2
BT-Cl

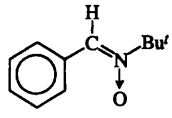

3
PBN

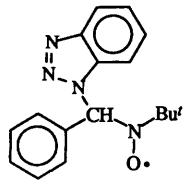

4

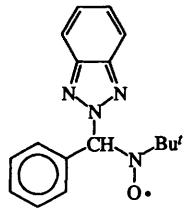

5

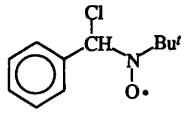

6

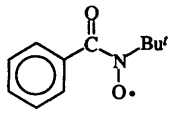

7

Results

Thermal reaction of *N*-chlorobenzotriazole 2 and PBN 3 in benzene

By mixing benzene solutions of **2** and PBN in the EPR cavity, the signals of the two spin adducts **4** and **5** could be recorded (Fig. 1; hfs coupling constants, see Table 1). The distinction

† IUPAC name: *N*-benzylidene-*tert*-butylamine *N*-oxide.

Table 1 Hfs constants of aminoxyl radicals detected

	Solvent	a^{N}/mT	$a^{N'}$/mT	a^{H}/mT	Other
4	Benzene	1.35	0.375	0.130	
	Dichloromethane	1.37	0.352	0.161	
	(^{2}H)Chloroform	1.38	0.346	0.141	
	Carbon tetrachloride	1.35	0.372	0.114	
	Benzotrifluoride	1.36	0.364	0.156	
	HFP[a]	1.49	0.275	0.316	
5	Benzene	1.32	0.42	0.29	$a^{N''}$ not resolved
	Dichloromethane	1.37	0.42	0.30	$a^{N''}$ not resolved
	(^{2}H)Chloroform	1.38	0.49	0.29	$a^{N''}$ not resolved
6	Benzene	1.25	0.080		a^{35Cl} 0.60
7	Benzene	0.79			
15	Benzene	1.53			

[a] 1,1,1,3,3,3-Hexafluoropropan-2-ol.

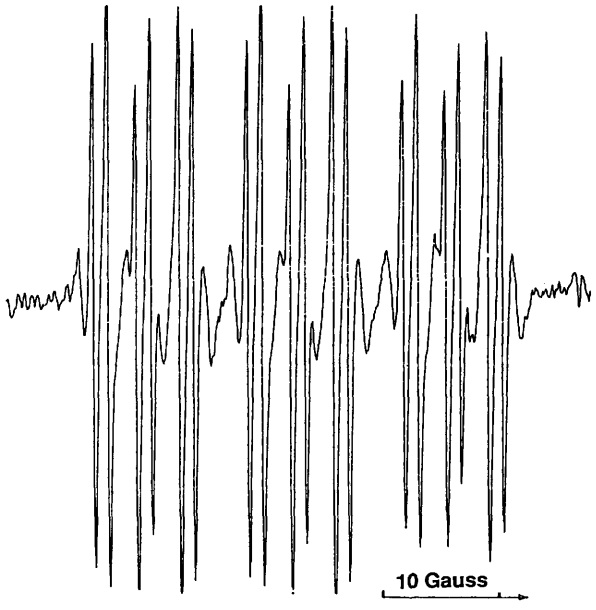

Fig. 1 EPR spectrum of the superimposition of signals **4** and **5**

between the 1- and 2-benzotriazolyl spin adduct structures was made on the basis of the linewidth of the signals; the spectrum with the broader signals was assumed to be derived from the 2-benzotriazolyl connected isomer, where coupling to the adjacent 1,3-nitrogen atoms of the benzotriazole ring would contribute more to line broadening than coupling to the single adjacent 2-nitrogen in the 1-benzotriazolyl spin adduct **4**. Despite much experimentation in a range of solvents, none of the signals of **4** or **5** could be further resolved.

A series of experiments was carried out in benzene with different concentrations of reagents and the evolution of the EPR signals was followed with time. The reaction carried out using the reagents in a 1:1 ratio immediately gave rise to the two EPR signals of spin adducts **4** and **5**, where the **4**:**5** ratio was *ca.* 10. The signal corresponding to **4** was the only one remaining after 2 h. Subsequently, this signal also began to decrease while the signal of the acylaminoxyl **7** started to appear; after 24 h, this was the only EPR signal remaining. Using BT–Cl and PBN in a 3:1 ratio the results were similar, while in the ratio 5:1, the chloro spin adduct **6** was observed at the beginning. After 30 min, this signal disappeared and the two signals corresponding to **4** and **5** clearly appeared, the former again being *ca.* 10 times more intense than the latter. After 2 h, both signals changed into the signal of aminoxyl **7**.

Thermal reaction of *N*-chlorobenzotriazole 2 and PBN 3 in dichloromethane

Reactions between BT–Cl and PBN in dichloromethane showed erratic behaviour with respect to the time development of the EPR signals of **4** and **5** when different samples of BT–Cl were used. Eventually it was realized that the reaction was autocatalytic, with benzotriazole (BT–H) as the catalytic species. Samples of BT–Cl inevitably contained small and varying amounts of benzotriazole, and the benzotriazole content increased upon storage. The catalytic effect of benzotriazole is clearly seen from the results shown in Fig. 2, where the time development of the **4** signal was recorded at different [BT–Cl], without or with benzotriazole added. The autocatalytic growth starts earlier and ends at a higher intensity level in the runs where benzotriazole has been added. During the period following the attainment of the maximum intensity of the signal of **4**, the acylaminoxyl **7** signal increases strongly (not shown in Fig. 2 for reasons of clarity).

A second series of experiments was made with the addition of tetrabutylammonium benzotriazolate as a possible catalyst instead of benzotriazole. However, only medium-intensity signals of **4** (but none of **5**) and **7** were seen, and they persisted almost unchanged for long periods. After addition of trifluoroacetic acid in an amount sufficient to neutralize the benzotriazolate present, autocatalytic growth of the **4** signal and rapid growth of the **7** signal ensued (Fig. 3), exactly as in the experiments with benzotriazole as the catalyst. The signal of **5** also appeared in low intensity upon addition of the acid.

If BT–H is the catalytic species and the reaction is of a radical nature, the regeneration of BT–H should occur *via* hydrogen atom abstraction by BT$^{\bullet}$ from a suitable species, in dichloromethane this is most likely from a solvent molecule. Neither BT–Cl nor PBN possesses any C–H bonds of low enough bond strength for this purpose. Thus autocatalytic behaviour should not be possible in benzene with its strong C–H bonds. Fig. 4 shows that this prediction is correct; in benzene the development of the **4** and **7** signals (filled and empty triangles, respectively) was slow and steady over a period of 70 min, even with BT–H added in a concentration (30 mM) which would initiate rapid growth after a few minutes in dichloromethane (Fig. 2). At that point, toluene (10% by volume) was added which immediately led to autocatalytic growth. The same behaviour was found when carbon tetrachloride was the solvent, but in this case with no extra BT–H added (Fig. 4). Again addition of toluene initiated rapid growth of the signals of **4** and **7** (filled and empty squares, respectively), although not as fast as in the benzene case due to the much lower [BT–H] present.

Thermal reaction of *N*-chlorobenzotriazole 2 and PBN 3 in acetonitrile

Reactions carried out in acetonitrile were extremely fast. Using the reagents in a 1:1 ratio, only the signal of **4** was observed at first; it disappeared in 5 min and after 10 min only the signal of the acylaminoxyl **7** was present. For the reactions using the reagents in 3:1 and 5:1 ratio, the signal of the chloro spin adduct **6** was observed at the beginning, but the results were essentially the

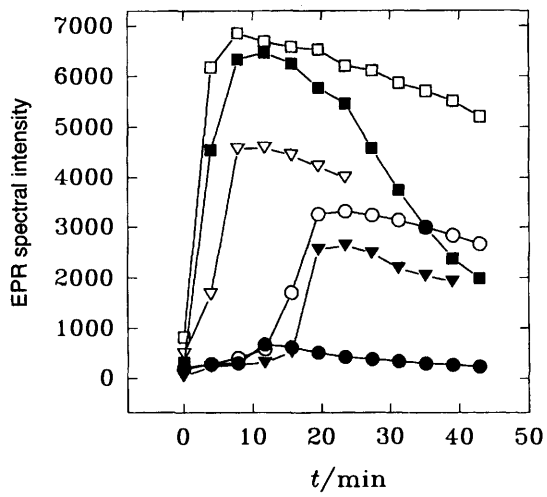

Fig. 2 Time dependence of the intensity of the 1-benzotriazolyl–PBN spin adduct signal from a dichloromethane solution of PBN (0.12 M) and *N*-chlorobenzotriazole (squares, 60 mM; triangles, 30 mM; circles 20 mM) without (filled symbols) or with (empty symbols) addition of benzotriazole (15 mM)

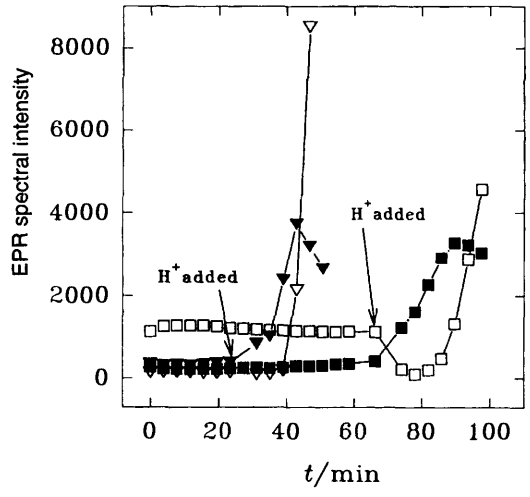

Fig. 3 Time dependence of the intensity of the 1-benzotriazolyl–PBN spin adduct (filled symbols) and acylaminoxyl (empty symbols) signals from solutions of PBN (0.12 M) and *N*-chlorobenzotriazole (60 mM) with tetrabutylammonium benzotriazolate (8 mM, triangles; 16 mM, squares). An equivalent amount of trifluoroacetic acid was added at times indicated by the arrows.

same as those observed for the reaction carried out in a 1 : 1 ratio.

Thermal reaction of *N*-chlorobenzotriazole 2 and PBN 3 in 1,1,1,3,3,3-hexafluoropropan-2-ol

Nucleophilic processes are drastically suppressed in 1,1,1,3,3,3-hexafluoropropan-2-ol (HFP), as recently shown for a range of nucleophile–radical cation reactions, including those of the benzotriazolate ion.[3] Thus any reaction sequence involving at least one nucleophilically controlled step should be strongly impeded in HFP. Fig. 5 shows that strong inhibition is observed for the BT–Cl–PBN reaction, even in the presence of an extremely high concentration of the catalyst BT–H, 0.14 M. The left curve corresponds to the dichloromethane reaction, with [BT–H] = 0.015 M.

The hfs coupling constants change significantly in HFP compared with the other solvents employed (Table 1). Similar effects were noted for other spin adducts.[3]

Photochemical reaction of *N*-chlorobenzotriazole 2 and PBN 3 in dichloromethane

The reaction between BT–Cl and PBN was strongly promoted

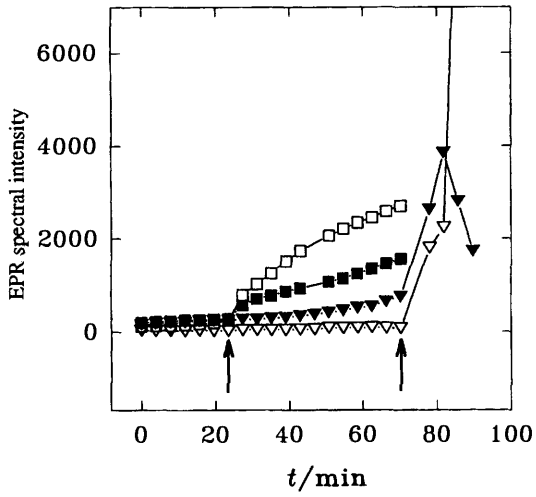

Fig. 4 Time dependence of the 1-benzotriazolyl–PBN spin adduct (filled symbols) and acylaminoxyl (empty symbols) signals from solutions of PBN (0.12 M) and *N*-chlorobenzotriazole (60 mM) in benzene with benzotriazole (30 mM, triangles) added or in carbon tetrachloride (squares). An amount of toluene corresponding to 10 vol% of the solution was added at times indicated by the arrows. Temperature, 22 °C.

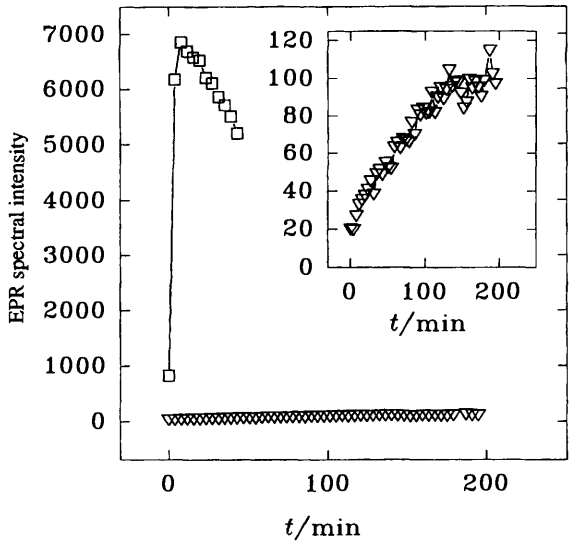

Fig. 5 Time development of the 1-BT–PBN$^{\bullet}$ (triangles) signal from a solution of PBN (0.12 M), BT–Cl (60 mM) and BT–H (0.14 M) in 1,1,1,3,3,3-hexafluoropropan-2-ol at 22 °C. As a comparison, one of the reactions shown in Fig. 2, carried out in dichloromethane under similar conditions (squares), except that [BT–H] was lower (15 mM), is included.

by UV light, presumably by the excitation of PBN (λ_{max} = 296 nm) to PBN*. The latter species is a strong reductant [redox potential of the singlet *vs.* electron acceptors ≈ -2.5 V (NHE)][4] which should react very rapidly with BT–Cl, a good acceptor (see below), with the formation of transient BT–Cl$^{\bullet -}$. After cleavage of the latter into the benzotriazolyl radical and chloride ion, a triad of PBN$^{\bullet +}$, BT$^{\bullet}$ and Cl^- provides the starting point for spin adduct formation.

Reactions were performed in dichloromethane with an excess of PBN over BT–Cl at 22, −20, −40 and −60 °C, cooling being helpful in bringing out the detailed order of events. The EPR signals were first monitored for about 30 min to check that no thermal autocatalysed process had been initiated. Then irradiation was performed for 5 min. Fig. 6(*a*) shows the time development of the signals of Cl–PBN$^{\bullet}$ **6**, 1-BT–PBN$^{\bullet}$ **4**, (2-BT–PBN$^{\bullet}$ **5** was also formed, but in much lower concentration) and the acylaminoxyl **7**. Both **4** and **6** increased strongly with irradiation and started to decay after the light was switched off. At this point, **7** started to build up. At −40 and −60 °C,

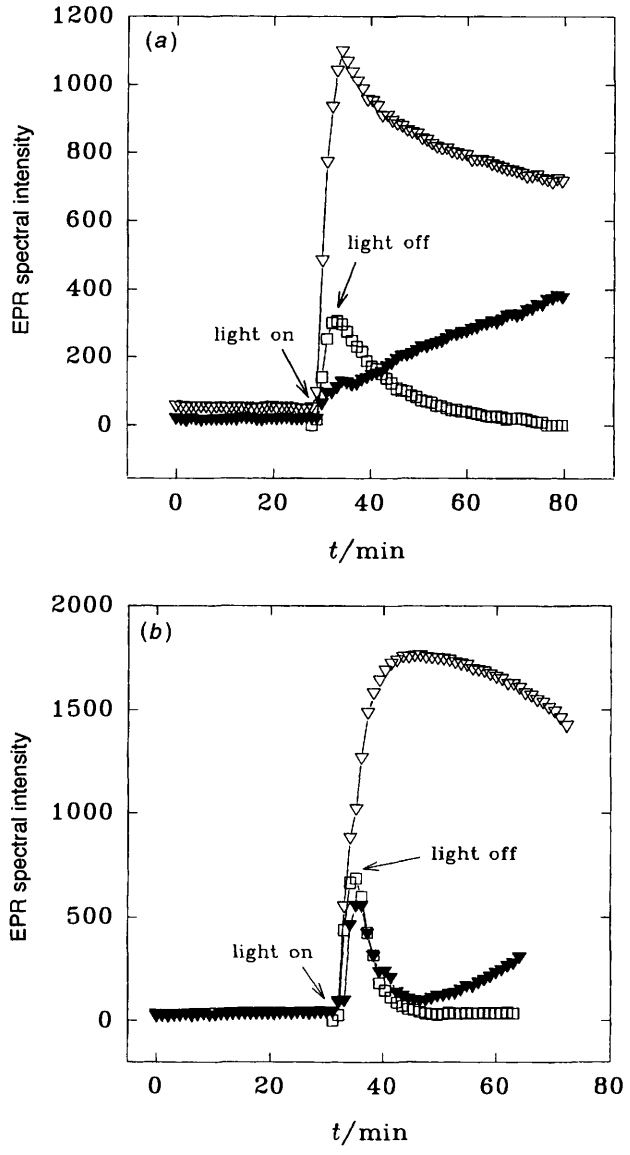

Fig. 6 Time development of Cl–PBN• (**6**, squares), 1-BT–PBN• (**4**, empty triangles) and acylaminoxyl (**7**, filled triangles) upon irradiation with UV light of a solution of PBN (0.10 M) and BT–Cl (20 mM) in (*a*) dichloromethane at −20 °C and (*b*) benzene at 22 °C

the similar behaviour of **4** and **6** was noticed, but the acylaminoxyl signal developed much more slowly; at 22 °C, the signal of **6** was less intense, and the acylaminoxyl signal increased faster.

Photochemical reaction of *N*-chlorobenzotriazole 2 and PBN 3 in benzene

Similar photolysis in benzene at 22 °C produced almost the same picture as in dichloromethane at −20 °C [Fig. 6(*b*)]. The proportion of 2-BT–PBN• **5** was somewhat larger in benzene.

Photochemical reaction of *N*-chlorobenzotriazole 2 and PBN 3 in HFP

Photolysis of PBN (0.12 M) and BT–Cl (0.060 M) in HFP produced a weak signal of **4** which disappeared rapidly after discontinuation of the irradiation, $k_{decay} \approx 0.08$ min^{-1}. No other signal was detectable, as expected in view of the fact that nucleophilic processes are strongly retarded in HFP.

Oxidation of a spin adduct by *N*-chlorobenzotriazole 2

Since spin adducts are reactive in redox reactions [oxidation potentials are in the range of 0.5–0.9 V (SCE)],[5] the possibility

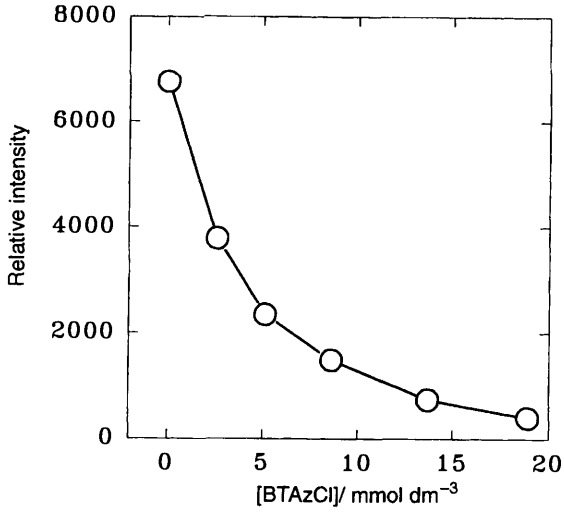

Fig. 7 Intensity of the succinimidyl-1,1-di-*tert*-butylethene spin adduct, generated by photolysis of a dichloromethane solution of 1,1-di-*tert*-butylethene (0.52 M) and *N*-chlorosuccinimide (0.10 M) in the presence of different [BT–Cl]

of further oxidation of spin adducts by good electron acceptors, such as BT–Cl, must be considered. For *N*-haloimides, another class of similar electron acceptors, this type of reaction has been demonstrated.[4]

Attempted trapping of the benzotriazolyl radical by photolysis of BT–Cl in the presence of 1,1-di-*tert*-butylethene in dichloromethane failed in the temperature range 22 to −40 °C. No signal of any kind was detectable. Since the succinimidyl radical is trapped by 1,1-di-*tert*-butylethene during photolysis of *N*-chlorosuccinimide and 1,1-di-*tert*-butylethene,[4] it became possible to study the effect of added BT–Cl upon the signal of the succinimidyl-1,1-di-*tert*-butylethene spin adduct. Fig. 7 shows that the signal intensity decreases to almost zero by the addition of 20 mM BT–Cl, signifying that BT–Cl (or products derived thereof) can destroy the primary spin adduct in sufficiently high concentration.

Electrochemistry

Cyclic voltammetry of a solution of tetrabutylammonium benzotriazolate in acetonitrile–tetrabutylammonium hexafluorophosphate (0.15 M) showed irreversible behaviour, E_{pa} of the benzotriazolate ion being 1.10 V (Ag/AgCl).

A fresh sample of *N*-chlorobenzotriazole under the same conditions displayed an irreversible reduction peak at 0.25 V (Ag/AgCl) and an oxidation peak at 1.15 V on the return scan.

Macroscale reaction of *N*-chlorobenzotriazole 2 and PBN 3

PBN and BT–Cl were allowed to react for 12 h in benzene at room temperature. Work-up of the reaction mixture gave the products reported in Scheme 1 in the yields listed in Table 2. Products **8**, **9**, **10** and **13** were identified by comparison with authentic samples.

The structures of compounds **11** and **12** were determined by X-ray crystallographic analysis and from their spectroscopic and analytical data. The structure of compound **14** was proposed by comparing its spectroscopic data with those of compounds **11** and **12**.

Molecular geometry of compounds 11 and 12

Selected bond distances, angles and torsion angles for compounds **11** and **12** are reported in Table 3. The arbitrary numbering scheme used in the crystal analysis is shown in Figs. 8 and 9 which represent perspective views of **11** and **12**, respectively.

The X-ray crystallographic analysis showed that compounds

Table 2 Products and yields of the reaction of BT–Cl and PBN in benzene at room temperature

Product	Yield (%)[a]
8	1.8
9	4.2
10	0.7
11	0.3
12	1.2
13	0.2
14	0.1

[a] Referred to PBN.

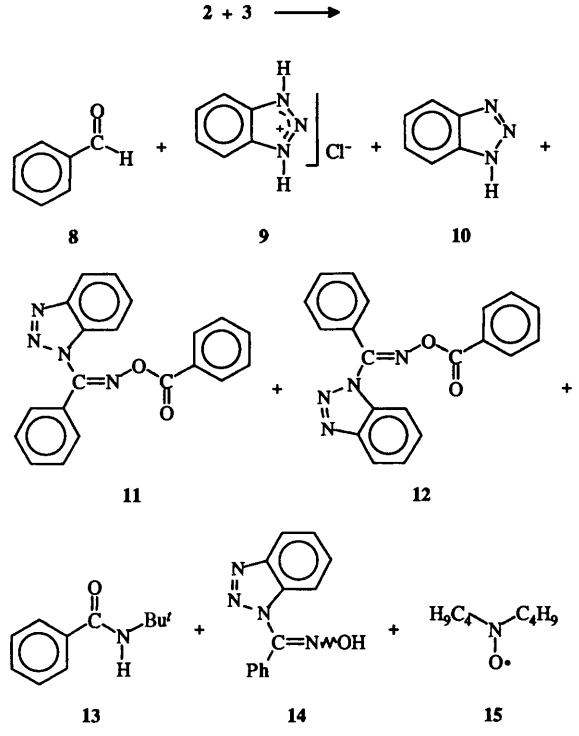

Scheme 1

11 and **12** are the isomers *Z* and *E* of benzotriazolyl phenyl ketone *O*-benzoyloxime, respectively.

The intramolecular bond lengths and angles, in line with the hybridization expected for the atoms involved and similar in the two compounds, revealed the presence of localized double bonds in the triazine ring [N(2)=N(3) = 1.300(12) and 1.288(3) Å], in the oxime moiety [N(4)=C(1) = 1.277(13) and 1.286(3) Å] and in the benzoyl group [O(1)=C(2) = 1.201(12) and 1.190(3) Å].

A comparison of the benzotriazine geometry with that reported in the literature[6] confirms that the values found for the N=N bond are consistent with a rigorous double bond character as defined by Pauling[7] and Bernstein[8] for compounds in which all the atoms are assumed to have sp^2 hybridization: it seems that the degree of delocalization of the N=N π bond in the five-membered ring, with consequent reduction in the differences of N–N bond lengths, can be influenced by the nature of the exocyclic substituent, being highest in the case of O and smallest in the case of C and H.

From the study of the conformational geometry by torsion angles and from the analysis of the planarity it is evident that the benzoyloxyimino moiety is nearly planar in the two isomers [the dihedral angles between the N(1), N(4), C(11) plane and the C(21)-ring one are 4.3(3) and 13.8(1)° and those between the N(1), N(4), C(11) and O(1), O(2), C(21) planes are 3.8(3) and 5.0(1)° in the *Z* and *E* isomers, respectively].

Table 3 Selected bond distances (Å), angles (°) and torsion angles (°) with esds in parentheses for the two isomers **11** and **12**

	(*Z*)-**11**	(*E*)-**12**
O(1)–C(2)	1.201(12)	1.190(3)
O(2)–N(4)	1.421(10)	1.422(3)
O(2)–C(2)	1.383(12)	1.364(3)
N(1)–N(2)	1.384(11)	1.381(3)
N(1)–C(1)	1.409(12)	1.416(3)
N(1)–C(9)	1.372(12)	1.377(3)
N(2)–N(3)	1.300(12)	1.288(3)
N(3)–C(4)	1.385(12)	1.382(3)
N(4)–C(1)	1.277(13)	1.286(3)
C(1)–C(11)	1.482(13)	1.476(3)
C(2)–C(21)	1.483(13)	1.481(3)
C(4)–C(9)	1.383(13)	1.389(3)
N(4)–O(2)–C(2)	114.0(7)	110.6(2)
N(2)–N(1)–C(1)	119.2(7)	119.8(2)
N(2)–N(1)–C(9)	109.0(7)	109.8(2)
C(1)–N(1)–C(9)	131.1(8)	130.0(2)
N(1)–N(2)–N(3)	108.3(7)	108.7(2)
N(2)–N(3)–C(4)	109.3(7)	108.7(2)
O(2)–N(4)–C(1)	109.1(8)	109.1(2)
N(1)–C(1)–N(4)	122.7(8)	112.0(2)
N(1)–C(1)–C(11)	117.7(8)	118.8(2)
N(4)–C(1)–C(11)	119.7(9)	129.2(2)
O(1)–C(2)–O(2)	122.5(9)	123.5(2)
O(1)–C(2)–C(21)	127.8(9)	125.7(2)
O(2)–C(2)–C(21)	109.7(8)	110.8(2)
N(3)–C(4)–C(9)	108.0(8)	109.3(2)
N(1)–C(9)–C(4)	105.4(8)	102.5(2)
N(4)–O(2)–C(2)–O(1)	−0.3(12)	−0.7(4)
N(4)–O(2)–C(2)–C(21)	178.1(7)	179.7(2)
C(2)–O(2)–N(4)–C(1)	175.5(8)	−174.8(2)
N(2)–N(1)–C(1)–C(11)	63.8(11)	−14.0(4)
N(2)–N(1)–C(1)–N(4)	−116.6(10)	166.1(2)
C(1)–N(1)–N(2)–N(3)	171.7(8)	−175.0(2)
O(2)–N(4)–C(1)–N(1)	3.4(12)	177.0(2)
O(2)–N(4)–C(1)–C(11)	−176.9(8)	−2.9(4)

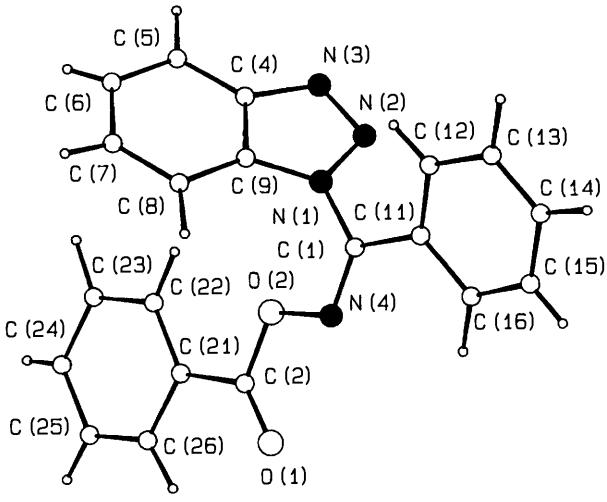

Fig. 8 Perspective view of (*Z*)-benzotriazolyl phenyl ketone *O*-benzoyloxime **11**

All the rings are planar within experimental error: the differences observed in the two compounds in the dihedral angles they form are interpreted in terms of steric hindrance.

Packing is consistent with van der Waals interactions.

Discussion

The experimental data obtained for the reaction of PBN with BT–Cl clearly show that these compounds react to afford the primary spin adducts **4**, **5** and **6**, which in time evolve to give the acylaminoxyl **7** and other diamagnetic products. The formation

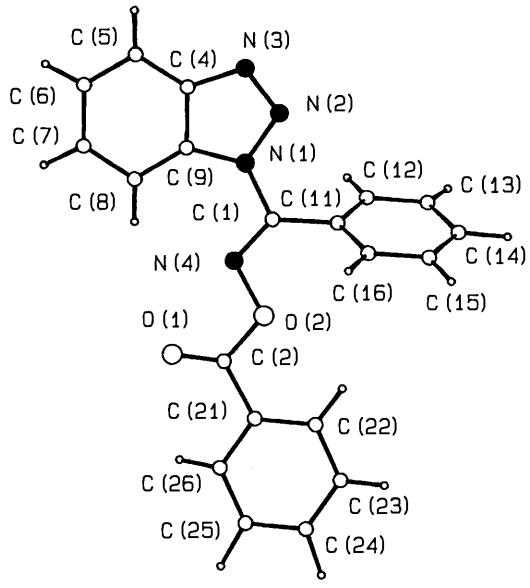

Fig. 9 Perspective view of (*E*)-benzotriazolyl phenyl ketone *O*-benzoyloxime **12**

of **4** and **5** can be explained on the basis of four mechanisms: (*i*) the trapping of the benzotriazolyl radical by PBN, which is the classical mechanism of spin trapping;[9] (*ii*) the nucleophilic addition[10] of benzotriazole **11** to PBN and subsequent one-electron oxidation;[11] (*iii*) the oxidation of PBN to the corresponding radical cation ($PBN^{\bullet+}$) and nucleophilic addition of benzotriazole **11**, which is the so-called inverted spin trapping (IST) mechanism;[12] (*iv*) the nucleophilic substitution of chlorine in Cl–$PBN^{\bullet}$ by BT–H.[13]

It is well known that BT–Cl is a good oxidant,[11] as confirmed here by its redox potential, 0.25 V (Ag/AgCl), which makes it a one-electron oxidant comparable with *N*-bromosuccinimide.[14] The anodic peak potential of the benzotriazolate ion, 1.1 V (Ag/AgCl), shows this nucleophile to be reactive towards one-electron oxidation and in fact comparable to the azide ion with $E^{\circ}(N_3^{\bullet}/N_3^{-})$ = 1.41 V (NHE).[15] The low value also ensures that the cleavage of the BT–Cl radical anion must give $BT^{\bullet}$ and Cl^{-} and not BT^{-} and $Cl^{\bullet}$ [eqns. (5) and (6)], in line with the behaviour of *N*-halosuccinimide radical anions.[16]

$$BT\text{–}Cl^{\bullet-} \longrightarrow BT^{\bullet} + Cl^{-} \quad (5)$$

$$BT\text{–}Cl^{\bullet-} \longrightarrow BT^{-} + Cl^{\bullet} \quad (6)$$

BT–Cl is also an effective chlorinating agent,[17] affording chlorinated derivatives and benzotriazole **11** when allowed to react with organic compounds. Radical chain mechanisms have been suggested for such chlorination.[18] However, in the macroscale reaction between PBN and BT–Cl no compounds chlorinated in the benzene ring or any other position of PBN were isolated. It is therefore not likely that a radical chain process is involved in the formation of **4** and **5**. On the other hand, a transient chlorinated product, Cl–$PBN^{\bullet}$ **6** does appear under most reactions conditions and must be accounted for (see below).

It is also unlikely that the reaction is initiated by an electron-transfer reaction between BT–Cl and PBN according to eqn. (7). In fact the reduction potential of BT–Cl (0.25 V *vs.* Ag/AgCl) and the oxidation potential of PBN (1.5 V *vs.* Ag/AgCl)[19] make this process endergonic by *ca.* 29 kcal mol^{-1}.‡ At least in solvents with relative permittivities > 10, such an electron transfer step is estimated to be very slow by the Marcus theory. However, considering that the reaction occurs between two neutral compounds to give two oppositely charged ions, the electrostatic correction term might compensate for the high endergonicity in a low permittivity solvent like benzene. This term is formally of the order −25 kcal mol^{-1} in benzene for the process of eqn. (7), assuming a distance of 5 Å between the two reactants in the transition state.[20] However, we are not convinced that this model can be extended to solvents at the extreme of low permittivity.

$$BT\text{–}Cl + PBN \longrightarrow BT\text{–}Cl^{\bullet-} + PBN^{\bullet+} \quad (7)$$

Instead, we suggest that the nucleophilic addition of BT–H,[21] inevitably present in traces in BT–Cl, to PBN constitutes the initial step of the reaction sequence leading to **4** and **5**. This step yields a redox reactive hydroxylamine [BT–PBN(H)] which is oxidized in a one-electron step by even relatively weak oxidants, *e.g.* BT–Cl. The benzotriazolyl radical formed can abstract a hydrogen atom from any suitable donor present, in which case the new BT–H molecule can enter the initiation reaction, *etc.* [eqns. (8)–(10)]. This scheme constitutes an autocatalysed

$$BT\text{–}H + PBN \rightleftharpoons BT\text{–}PBN(H) \quad (8)$$

$$BT\text{–}PBN(H) + BT\text{–}Cl \longrightarrow BT\text{–}PBN^{\bullet} + HCl + BT^{\bullet} \quad (9)$$

$$BT^{\bullet} + H\text{–}C \longrightarrow BT\text{–}H + C^{\bullet} \quad (10)$$

process which is amply documented in Figs. 2–4, where the solvent dichloromethane is the H atom donating species of eqn. (10). In benzene and carbon tetrachloride, the solvent cannot fulfil this role, and no autocatalytic behaviour is seen until an H atom donor (toluene) is deliberately added.

The fact that tetrabutylammonium benzotriazolate does not sustain the autocatalytic behaviour may at first seem surprising, but must be due to an unfavourable equilibrium of eqn. (11). If

$$BT^{-} + PBN \rightleftharpoons BT\text{–}PBN^{-} \quad (11)$$

this is strongly displaced to the left, the second-order reaction between the hydroxylamine anion and BT–Cl becomes very slow.

HFP is a unique solvent in its ability to suppress nucleophilic mechanisms.[3,22] Already 10% HFP in dichloromethane prevents the inverted spin trapping[5] of benzotriazolate ion by $PBN^{\bullet+}$, and the very weak signal observed in HFP (Fig. 5) under conditions which would have sustained a very fast autocatalysis in dichloromethane is in line with the assumption that the nucleophilic initiation reaction [eqn. (8)] has been strongly inhibited.

The photochemical generation of **4**, **5** and **7** (Fig. 6) is efficient and leads to strong signals. Here the mechanism presumably involves a photoelectron transfer induced reaction, involving excitation of PBN to its singlet or triplet state which in either case should very rapidly transfer an electron to the acceptor BT–Cl [eqns. (12) and (13)]. The combination of $PBN^{\bullet+}$ and Cl^{-} will give Cl–$PBN^{\bullet}$ **6** [reaction (14)],[4,12]

$$PBN \longrightarrow PBN^{*} \quad (12)$$

$$PBN^{*} + BT\text{–}Cl \longrightarrow PBN^{\bullet+} + BT^{\bullet} + Cl^{-} \quad (13)$$

$$PBN^{\bullet+} + Cl^{-} \longrightarrow Cl\text{–}PBN^{\bullet} \quad (14)$$

whereas $BT^{\bullet}$ may either add to PBN as such or initiate the autocatalytic mechanism provided an H atom donor is present.

Most experiments demonstrate that the first spin adducts formed are **4**, **5** (Fig. 2) and **6**. The signal of the chloro spin adduct **6** disappeared rapidly, whereas those of **4** and **5** decayed more slowly. At the same time the signal of the acylaminoxyl **7** increased in intensity and was the only signal present after 20 h.

‡ 1 cal = 4.184 J.

Because the spin adduct **5** was never observed when the reaction was carried out under 'nucleophilic conditions' (PBN + BTH + a weak oxidant), it was assumed that its formation may be ascribed to the spin trapping of the benzotriazolyl radical.

The chloro spin adduct **6** was predominantly observed in thermal reactions with an excess of BT–Cl in benzene, dichloromethane or acetonitrile, and under photolytic conditions. In our opinion, its formation may occur in all the studied reactions; it is a reactive aminoxyl radical which easily undergoes nucleophilic substitution [13] and thus may be transformed either into **4** or to the acylaminoxyl **7**. The spin adduct **6** could also be formed in ways other than the one indicated above [reaction (13) and (14)]: (*i*) by spin trapping of a chlorine atom formed photochemically by homolytic cleavage of BT–Cl or (*ii*) by addition of HCl [23] to PBN [see reaction (15)] and subsequent oxidation according to reaction (16). As a

$$\text{PBN} + \text{HCl} \longrightarrow \text{Ph(Cl)CH–N(OH)Bu}^t \quad (15)$$

$$\text{Ph(Cl)CH–N(OH)Bu}^t + \text{Oxidant} \longrightarrow \text{Ph(Cl)CH–N(O}^\bullet\text{)Bu}^t \quad (16)$$

matter of fact, bubbling dried HCl into a benzene solution of PBN and oxidizing afterwards with PbO_2, the signal of acylaminoxyl **7** was observed; in our opinion the latter was formed through the intermediate formation of the chlorine spin adduct.

Even if several ways have been proposed for the transformation of chloro adduct **6** into the acylaminoxyl by different researchers,[10b,12] the formation of the acylaminoxyl can also be explained by the interaction of the chloro adduct **6** and PBN itself as shown in reaction (17).[24]

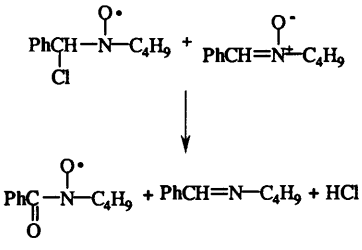

(17)

The macroscale reaction between BT–Cl and PBN performed in benzene at room temperature confirms the results obtained in the EPR spectral experiments. The formation of benzotriazole **10** and its hydrochloride derivative **9** as the major products indicate that BT–Cl is involved in an electron-transfer process according to the discussion above.

The presence of benzaldehyde **8** among the reaction products could indirectly confirm the formation of *N*-benzylidene-*tert*-butylamine [see reaction (17)], which may be the origin of the benzaldehyde. This imino derivative, which was not isolated, could add hydrogen chloride and the chloro adduct leading to the formation of compound **13** according to the sequence shown in Scheme 2.

The isolation and identification of compounds **11**, **12** and **14** indicate that the spin adduct **4** is predominantly formed by bonding of the benzotriazolyl group PBN *via* N-1. The disappearance of the signals of the spin adduct **4** could be due to an oxidative process (BT–Cl is a good candidate for this task, as demonstrated by the results of Fig. 7) leading to the formation of a nitrone which might react with benzaldehyde to give compounds **11** and **12** (see Scheme 3).

In order to obtain some experimental support for this proposal an experiment to simulate this reaction was carried out by reacting PBN and benzaldehyde in benzene in the presence of PbO_2, but the expected product was not isolated.

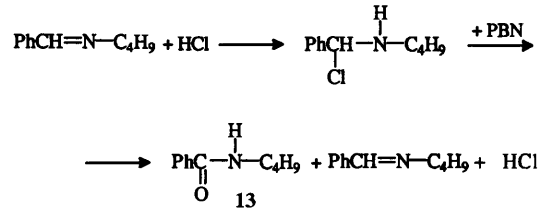

Scheme 2

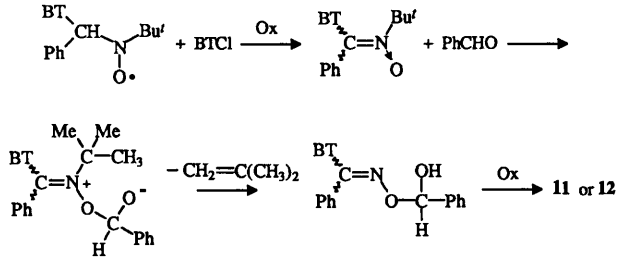

Scheme 3

Conclusions

The reactions of BT–Cl with indoles gave evidence for an electron-transfer process involving radicals as intermediates.[1] In order to better understand this reaction, experiments were carried out by reacting 1-methyl-2-phenylindole with BT–Cl in the presence of PBN with the aim being to trap intermediate radicals. The data described above show that BT–Cl reacts with PBN by itself, which leads to the generation of benzotriazolyl and chloro spin adducts, whose formation may involve more than one mechanism (see Discussion section). These results demonstrate the limits of PBN as a spin trap for the investigation of reaction mechanisms.

Experimental

Melting points were measured on an Electrothermal Melting Point Apparatus and are uncorrected. IR spectra were recorded by a Perkin-Elmer model 298 spectrophotometer. ^1H and ^{13}C NMR spectra were recorded in $CDCl_3$ on a Varian Gemini 200 spectrometer and chemical shifts (in ppm) were reported downfield from TMS. *J* Values are given in Hz. Mass spectra were recorded in EI^+ mode on a Carlo Erba QMD 1000 GLC/MS spectrometer equipped with a direct probe apparatus. EPR spectra were either recorded on the Upgrade Version ESP 3220-200SH of a Bruker ER-200D spectrometer, equipped with a photolysis cavity, or on a Varian E4 spectrometer. The light source was the 50 W high pressure Hg lamp from Bruker (ER 202). *N*-Chlorobenzotriazole [25] and tetrabutylammonium benzotriazolate [26] were prepared as reported in the literature. All other compounds were purchased from Aldrich. All solvents were Fluka RP-ACS or Merck UVASOL quality.

Reactions of PBN and BT–Cl performed in the EPR cavity

EPR spectra from the time-resolved reactions were recorded on the Bruker instrument as described.[4] EPR spectra from the Varian instrument were recorded with solutions contained in an inverted U-cell, similar to that described by Russel *et al.*[27] Solutions of the reagents in the appropriate concentrations were separately introduced into the two legs of the inverted cell. After degassing with nitrogen, the solutions were mixed and the U-cell mounted into the EPR cavity (version for aqueous solutions). The signals were recorded starting 2–3 min after mixing and their evolution was followed for 24 h in some cases.

Table 4 Experimental data for the X-ray diffraction studies[a] on crystalline compounds **11** and **12**

Compound	(*Z*)-**11**	(*E*)-**12**
Formula	$C_{20}H_{14}N_4O_2$	$C_{20}H_{14}N_4O_2$
Crystal habit	Tabular prism	Elongat. prism
Crystal colour	Colourless	Colourless
Molecular weight	342.4	342.4
F(000)	712	712
Crystal system	Monoclinic	Monoclinic
Space group	$P2_1/c$	$P2_1/c$
Cell parameters at 295 K[b]		
a/Å	9.835(3)	7.042(2)
b/Å	7.444(2)	20.628(4)
c/Å	23.207(4)	11.788(3)
α; β; γ/degrees	90; 96.5(1); 90	90; 99.6(1); 90
V/Å^3	1688.1(8)	1688.4(9)
Z	4	4
D_c/g cm^{-3}	1.35	1.35
Crystal dim./mm	0.02 × 0.12 × 0.21	0.23 × 0.14 × 0.48
μ/cm^{-1}	7.4	7.4
Diffractometer	Siemens AED	Siemens AED
Scan type	ω–2θ	ω–2θ
Scan width/degrees	$(\theta - 0.6)$–$[\theta + (0.6 + \Delta\theta)]$ $\Delta\theta = [(\lambda\alpha_2 - \lambda\alpha_1)/\lambda] \tan\theta$	$(\theta - 0.6)$–$[\theta + (0.6 + \Delta\theta)]$
Radiation	Ni-filtered Cu-Kα; λ = 1.541 78 Å	Ni-filtered Cu-Kα; λ = 1.541 78 Å
θ Range coll./degrees	3–70	3–70
Unique total data	3510	3439
Criterion of obs.	$I > 2\sigma(I)$	$I > 2\sigma(I)$
Unique observed data	827	2145
No. of refined par.	291	291
Absorption	No correction applied	No correction applied
Solution	Direct methods	Direct methods
H atoms	Located in ΔF map and isotropically refined	Located in ΔF map and isotropically refined
R ($\Sigma\lvert\Delta F\rvert/\Sigma\lvert F_o\rvert$)	0.047	0.052
R_w $[\Sigma_w(\Delta F^2)^2/\Sigma_w(F_o^2)^2]$	0.046	0.060
Largest shift (esd)	0.2	0.4
Largest peak/e Å^{-3}	0.17	0.17

[a] Computer and programs: ENCORE E91, SHELXS86,[28] SHELX76,[29] PARST.[30b] Unit cell parameters were obtained by least-squares analysis of the setting angles of 30 carefully centred reflections chosen from the diverse region of reciprocal space.

Macroscale reaction of PBN with BT–Cl

BT–Cl (0.94 g, 6 mmol in 10 ml of benzene) was added at room temperature and with stirring to a solution of PBN (1.062 g, 6 mmol in 10 ml benzene). In the first 2 h no changes were observed. After 12 h a white precipitate had been formed and the solution was pale yellow. The reaction mixture was examined by EPR spectroscopy giving the signal of the acylaminoxyl **7** and then worked up: the precipitate was filtered off (40 mg of benzotriazole hydrochloride **9**) and the solution chromatographed on preparative TLC eluting with cyclohexane–ethyl acetate 8:2. Products were isolated in the following order (from the top): benzaldehyde **8**, benzotriazole **10**, (*Z*)-benzoyloxime **11**, (*E*)-benzoyloxime **12**, *N*-*tert*-butylbenzoylamide **13** and oxime **14** (yields are reported in Table 2). In some portions of the filtrate the EPR signal of di-*tert*-butyl aminoxyl **15** was recorded.

Spectroscopic data for compounds 11–14

Compound 11. Mp 168–170 °C; ν(Nujol)/cm^{-1} 1745, 1625, 1410, 1375, 1260, 1240, 1055, 980, 945 and 700; δ_H($CDCl_3$) 7.46 (2 H, m, arom), 7.54–7.79 (8 H, m, arom), 7.91 (2 H, m, arom), 8.17 (1 H, dt, *J* 8.3 and 1.1, arom) and 8.60 (1 H, dt, *J* 8.3 and 1.1, arom); δ_C($CDCl_3$) 115.6, 120.6, 126.4, 127.6, 128.4, 129, 129.2, 130.2, 130.4, 130.5, 132.9, 134.2, 147.7, 158.4 and 163.7; *m*/*z* 342 (M^+, 20%), 192 (100), 179 (40), 152 (17) and 105 (97).

Compound 12. Mp 129–131 °C; ν(Nujol)/cm^{-1} 1770, 1600, 1405, 1375, 1325, 1080, 1060, 1025, 980, 860 and 700; δ_H($CDCl_3$) 7.29 (2 H, m, arom), 7.35–7.70 (11 H, m, arom) and 8.25 (1 H, m, arom); δ_C($CDCl_3$) 112, 121.1, 125.6, 127.8, 129, 129.5, 129.7, 129.9, 130.3, 133.3, 133.7, 134.3, 145.6, 150.5 and 163; *m*/*z* 342 (M^+, 24%), 192 (100), 179 (83), 152 (43) and 105 (97).

Compound 13. Mp 124–126 °C; ν(Nujol)/cm^{-1} 3320, 1635, 1580, 1310, 1215, 1140 and 865; δ_H($CDCl_3$) 1.47 (9 H, s, Bu^t), 5.95 (1 H, broad, N*H*), 7.42 (3 H, m, arom) and 7.72 (2 H, m, arom); *m*/*z* 177 (M^+, 84%), 162 (88), 122 (89) and 105 (100).

Compound 14. ν(Nujol)/cm^{-1} 3170, 1285, 1160, 1140, 1100, 1000, 950, 760, 740 and 690; δ_H($CDCl_3$) 7.35–7.66 (7 H, m, arom), 7.88 (1 H, dt, *J* 8.1 and 1.24, arom), 8.16 (1 H, m, arom) and 8.45 (1 H, br, NO*H*); δ_C($CDCl_3$) 112.3, 113.5, 120.6, 125.1, 125.6, 127.8, 128.9, 129.3, 130.3, 131.5, 131.6, 145.4 and 146.4; *m*/*z* 239 ($M^+ + 1$, 16%), 208 (100), 192 (98), 178 (50), 166 (41) and 152 (35).

Crystal structure of (*Z*)- and (*E*)-benzotriazolyl phenyl ketone *O*-benzoyloxime 11 and 12

Table 4 shows the experimental and crystallographic data for the *Z* and *E* isomers. The intensities I_{hkl} were determined by analysing the reflection profiles.[31] Atomic scattering factors were from the International Tables for X-Ray Crystallography.[32] Bibliographic searches were carried out using the Cambridge Structural Database Files through the Servizio Italiano di Diffusione Dati Cristallografici, Parma, Italy.

Atomic fractional coordinates, thermal parameters and structure factors have been deposited at the Cambridge Crystallographic Data Centre. For details of the CCDC deposition scheme, see 'Instruction for Authors', *J. Chem. Soc., Perkin Trans. 2*, 1996, Issue No. 1. Any request to the CCDC for this material should quote the full literature citation and the reference number 188/7.

Acknowledgements

Financial support from the Italian Ministero dell'Università e della Ricerca Scientifica e Tecnologica (MURST) (to L. G.), the Swedish Natural Science Research Council (to L. E.) and the Knut and Alice Wallenberg Foundation (to L. E.) is gratefully acknowledged.

References

1 (*a*) P. Carloni, L. Eberson, L. Greci, P. Stipa and G. Tosi, *J. Chem. Soc., Perkin Trans. 2*, 1991, 1779; (*b*) R. Andruzzi, C. Berti, L. Greci and A. Trazza, *J. Org. Chem.*, 1982, **47**, 4895.
2 (*a*) E. G. Janzen, *Acc. Chem. Res.*, 1971, **4**, 31; (*b*) M. J. Perkins, *Adv. Phys. Org. Chem.*, 1980, **17**, 1; (*c*) V. Zubarev and O. Brede, *J. Chem. Soc., Perkin Trans. 2*, 1994, 1821.
3 L. Eberson, M. P. Hartshorn and O. Persson, *J. Chem. Soc., Perkin Trans. 2*, 1996, 141.
4 L. Eberson, J. Lind and G. Merenyi, *J. Chem. Soc., Perkin Trans. 2*, 1994, 1181.
5 L. B. Volodarsky, *Imidazoline Nitroxides*, CRC Press, Inc., Boca Raton, Florida, 1988, vol. 1, p. 175.
6 (*a*) A. Escande, J. L. Galign and J. Lapasset, *Acta Crystallogr., Sect. B*, 1974, **30**, 1490; (*b*) R. Bosch, G. Jung and W. Winter, *Acta Crystallogr., Sect. C*, 1983, **39**, 1089; (*c*) A. R. Katritzky, J. Wu, L. Wrobel, S. Rachwal and P. J. Steel, *Acta Chem. Scand.*, 1993, **47**, 167.
7 L. Pauling, *The Nature of the Chemical Bond*, 3rd edn., Cornell University Press, Ithaca, 1960, pp. 232–240.
8 H. J. Bernstein, *Trans. Faraday Soc.*, 1961, **57**, 1649.
9 (*a*) M. Iwamura and N. Inamoto, *Bull. Chem. Soc. Jpn.*, 1967, **40**, 702; (*b*) 1970, **43**, 856; (*c*) O. W. Maender and E. G. Janzen, *J. Org. Chem.*, 1969, **34**, 4072.
10 (*a*) H. G. Aurich, S. K. Duggal, P. Hohlein, H.-G. Klingelhofer and W. Weiss, *Chem. Ber.*, 1981, **114**, 2440; (*b*) E. G. Janzen and B. J. Blackburn, *J. Am. Chem. Soc.*, 1969, **91**, 4481; (*c*) M. Colonna, L. Greci and L. Marchetti, *Tetrahedron*, 1975, **31**, 1745.
11 *N*-Chlorobenzotriazole may be the most important oxidant present in solution suitable for this oxidation.
12 L. Eberson, *J. Chem. Soc., Perkin Trans. 2*, 1992, 1807.
13 M. J. Davies, B. C. Gilbert, J. K. Stell and A. C. Whitwood, *J. Chem. Soc., Perkin Trans. 2*, 1992, 333.
14 L. Eberson, J. E. Barry, M. Finkelstein, W. M. Moore and S. D. Ross, *Acta Chem. Scand., Ser. B*, 1986, **40**, 283.
15 M. S. Ram and D. M. Stanbury, *Inorg. Chem.*, 1995, **24**, 4234.
16 J. Lind, X. Shen, T. E. Eriksen, G. Merenyi and L. Eberson, *J. Am. Chem. Soc.*, 1991, **113**, 4629; J. Lind, M. Jonsson, T. E. Eriksen, G. Merenyi and L. Eberson, *J. Phys. Chem.*, 1993, **97**, 1610.
17 (*a*) K. V. Lichman, *J. Chem. Soc. C*, 1971, 2539; (*b*) P. M. Bowyer, D. H. Iles and A. Ledwith, *J. Chem. Soc. C*, 1971, 2775; (*c*) M. Cinquini and S. Colonna, *Synthesis*, 1972, 259.
18 (*a*) C. W. Rees and R. C. Storr, *J. Chem. Soc. C*, 1969, 1474; (*b*) W. D. Kingsbury and C. R. Johnson, *J. Chem. Soc., Chem. Commun.*, 1969, 65.
19 G. L. McIntire, H. N. Blount, H. J. Stronks, R. V. Shetty and E. G. Janzen, *J. Phys Chem.*, 1980, **84**, 916.
20 For calculation of the electrostatic term, see: L. Eberson, *Electron Transfer Reactions in Organic Chemistry*, Springer-Verlag, Heidelberg, 1987.
21 P. Carloni, L. Eberson L. Greci and P. Stipa, unpublished results.
22 (*a*) L. Eberson, M. P. Hartshorn, F. Radner and O. Persson, *J. Chem. Soc., Chem. Commun.*, 1996, 215; (*b*) L. Eberson, M. P. Hartshorn, F. Radner and O. Persson, in *Res. Chem. Intermed.*, 1996, in the press; (*c*) L. Eberson, M. P. Hartshorn and O. Persson, *Angew. Chem.*, 1995, **107**, 2417.
23 M. Ogata, H. Kano and K. Tori, *Chem. Pharm. Bull.*, 1963, **11**, 1527.
24 E. G. Janzen, G. Chen, T. M. Bray, L. A. Reinke, J. L. Poyer and P. B. McCay, *J. Chem. Soc., Perkin Trans. 2*, 1993, 1983.
25 C. W. Rees and R. C. Storr, *J. Chem. Soc., Chem. Commun.*, 1968, 1305.
26 L. Eberson and L. Jonsson, *Acta Chem. Scand., Ser. B*, 1986, **40**, 79.
27 G. A. Russel, E. G. Janzen and E. T. Strom, *J. Am. Chem. Soc.*, 1964, **86**, 1806.
28 G. M. Sheldrick, SHELXS86, Program for the Solution of Crystal Structures, University of Göttingen, 1986.
29 G. M. Sheldrick, SHELX76, System of Computer Programs for Crystal Structure Determination, University of Cambridge, 1976.
30 M. Nardelli, *Comput. Chem.*, 1983, **7**, 95.
31 M. S. Lehmann and F. K. Larsen, *Acta Crystallogr., Sect. A*, 1974, **30**, 580.
32 *International Tables for X-Ray Crystallography*, Kynoch Press, Birmingam, 1974, vol. IV.

Paper 6/00907G
Received 7*th February* 1996
Accepted 23*rd February* 1996